Available online at www.sciencedirect.com

ScienceDirect

Mendeleev Commun., 2020, **30**, 525–526

Mendeleev Communications

Compaction of nanosilicon pellets and sol-deposited films *via* high-vacuum annealing

Alexander A. Vinokurov,*[a] Sergei S. Bubenov,[a] Nikolay N. Kononov,[b] Tatiana A. Kuznetsova[a] and Sergey G. Dorofeev[a]

[a] *Department of Chemistry, M. V. Lomonosov Moscow State University, 119991 Moscow, Russian Federation. Fax: +7 495 939 0998; e-mail: vinokuroff.aa@gmail.com*

[b] *A. M. Prokhorov General Physics Institute, Russian Academy of Sciences, 119991 Moscow, Russian Federation. Fax: +7 499 503 8723*

DOI: 10.1016/j.mencom.2020.07.041

The density of nanoparticle composites influences their electronic properties. We used X-ray fluorescence- and UV-VIS spectroscopy-based techniques to demonstrate, that sol-processed nanosilicon films were friable, however their density was improved up to ~1 g cm^{-3} with high-vacuum annealing due to compaction of the nanosilicon particle packing. According to SEM data, the size and shape of nanoparticles remained unchanged after the annealing, except for a silicon whisker growth observed at 1000 °C.

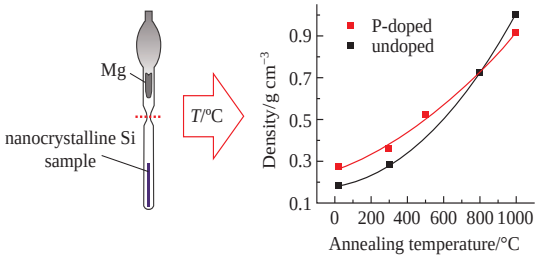

Keywords: nanosilicon sol, nanosilicon film, film density, spin coating, annealing, compaction.

Density influences many functional properties of materials. For thin films, density is measured by weighing[1] as well as typically by more sophisticated methods, including ones based on laser-generated surface acoustic waves,[2] ellipsometry,[3] spectrophotometry,[4] Rutherford backscattering of charged particles,[5] X-ray absorption or fluorescence,[6,7] electron energy loss spectra[8] and angular dependence of specular X-ray reflectivity.[9]

For films of silicon nanocrystals produced by chemical vapor deposition, the density constitutes ~30% of that of bulk silicon.[10] The conditions of other gas-phase approaches, including aerosol impaction or supersonic aerosol jet deposition, can be varied to produce films with a relative density range from ~5% in dendrite-like structures[3,11] to ~60% in random close packing of particles.[12,13] In general, for efficient electronic transport through a network, high fraction of conducting material is essential.[14] For semiconductor nanoparticles, solution processing typically leads to lower fractions of conducting particles in films at least due to a surface passivation,[15] therefore new techniques of compacting the solution-processed nanoparticle films are sought for. The purpose of this work was to determine the density of nanosilicon films prepared from sols and to explore compaction of these films.

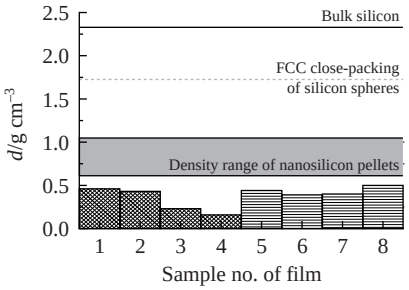

Figure 1 Density of nonannealed nanosilicon pellets and eight samples of films deposited from sols by (1–4) spin coating and (5–8) centrifugation.

Figure 1 demonstrates the densities of nanosilicon pellets as well as films deposited by spin-coating (SP-films) and centrifugation (C-films) techniques.† The film densities were 0.2–0.5 g cm^{-3}, whereas the density of nanosilicon pellets varied in a range of 0.61–1.05 g cm^{-3}. For comparison, the densities of face-centered cubic (FCC) close-packed silicon spheres (1.725 g cm^{-3}) and bulk silicon (2.330 g cm^{-3}) are given in Figure 1. We assumed that both nanosilicon film and pellets contained a large number of cavities, as the packing of silicon particles was friable.

This statement is based on the SEM microphotographs‡ of nanosilicon pellets, SP-films and C-films (Figures 2 and 3). The films were loose and highly porous over the entire thickness, with large cavities that were connected by foramens, whereas in

† We used pure silicon nanoparticles with 10–15 nm diameter, which had been synthesized by pyrolysis of monosilane[16] as well as silicon nanoparticles doped with 0.24 at% phosphorus.[17] Other commercial chemicals were used without additional purification: SiO (high purity), Ti (99%), Al (99.9999%), Au (99.99%), Mg (99.99%), argon (high purity) and C_2H_5OH (95%).

Nanosilicon pellets were pressed at 4 kbar using steel press forms of 3 and 6 mm diameters. Sols were prepared by dispersion of nanosilicon powder in ethanol employing an ultrasonic bath, the sol concentration was ~0.13 mg ml^{-1}. Doped silicon nanoparticles were preliminarily etched with concentrated hydrofluoric acid to dissolve surface silicon oxide. Sols were used for fabrication of films on glass and thermooxidized silicon substrates. Glass substrates were processed by argon plasma for better wettability. A gold layer was deposited on silicon substrates before the film deposition to make possible further measurement of the surface density of films (see Online Supplementary Materials). Spin coating was performed using a KW-4A spin coater (Chemat Technology, USA) in the following way. Dripping of the sol onto the substrate was followed by solvent evaporation at 1000 rpm for 1 min as well as the final alignment and drying at 6000 rpm for 2 min. This procedure was repeated up to 10 times to produce a desired film thickness. Centrifugation of nanosilicon sols was carried out using a Hettich EBA-21 centrifuge (Germany) at 12500 g for 15 min or at 18000 g for 5 min. This deposition method allows a control of film thickness by varying the sol concentration.

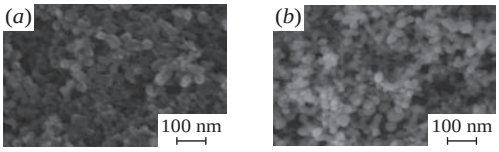

Figure 2 Typical SEM image of (*a*) nonannealed nanosilicon pellet and (*b*) SP-film.

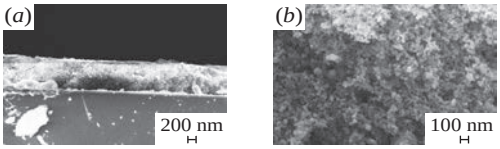

Figure 3 SEM images of nanosilicon C-films: (*a*) end cleavage and (*b*) top view.

pellets the packing of nanosilicon particles was closer and the cavities were smaller.

To improve the packing efficiency, nanosilicon pellets were annealed at different temperatures[§] and their density was determined (Table 1). Annealing at 500 and 800 °C hardly affected the density, whereas treatment at 1000 °C led to its increase by 1–10%. According to SEM data, the morphology of pellets remained unchanged upon annealing.

Volumetric density of annealed undoped and doped nanosilicon C-films was calculated from their surface density and thickness (see Table 1). Increase in the annealing temperature led to a steady growth of volumetric density for undoped C-film up to 1.00 g cm^{-3}. An increase in the density of undoped films was higher than that of the doped ones due to the crystallization of amorphous silicon. For P-doped films, the amorphous layer had crystallized in annealing during the doping procedure.[17]

SEM images of C-films did not reveal any difference between the initial samples and the annealed ones except for the film annealed at 1000 °C. For this sample, there were numerous silicon whiskers, which had grown through the film (Figure 4). The growth of silicon whiskers *in vacuo* at 1200 °C had been described,[18] but in our experiment the temperature was lower by 200 °C. From SEM images, we can conclude that particle size and shape are not noticeably affected by annealing.

In summary, we have explored the volumetric density of nanosilicon pellets and sol-deposited films. The sol processed

Films thickness was determined using a TalyStep profilometer (Tailor-Hobbson, USA). Nanosilicon films were friable and the measuring needle was drowning, therefore the direct observations were not possible. To ensure the measurement, a 200 nm Ti layer was deposited by thermal spray technique *in vacuo* after scratching the films. This layer provided the necessary toughness to the films and did not affect the measurement results. The data were averaged over five determinations and diverged from direct SEM measurements by less than 20%.

Volumetric density of the nanosilicon films was derived from their surface density. The surface density of relatively thick nanosilicon films (2–20 μm), which absorbed the M-series radiation of gold, was calculated by absorption of X-ray fluorescence (XRF) of the gold mark deposited on the substrates prior to introduction of nanosilicon. For optically transparent 0.2–3 μm films deposited on glass substrates, the surface density was determined using optical absorption. The XRF and optical absorption spectra were obtained using a Bruker M1 Mistral X-ray spectrometer and a Varian Cary 50 spectrometer (USA), respectively (see Online Supplementary Materials).

[‡] Film morphology was investigated using a Carl Zeiss Supra 40 scanning electron microscope (Germany) at accelerating voltage 10 kV and resolution 1.5 nm.

[§] Annealing of nanosilicon pellets and films was performed in quartz ampoules evacuated to 1×10^{-2} Torr. Sealed ampoules were initially annealed with a magnesium getter at 120 °C for the removal of residual oxygen and water. Then they were separated from the getter and finally annealed at 300–1000 °C for 2 h (see Online Supplementary Materials).

Table 1 Density of nanocrystalline silicon pellets (6 mm in diameter pressed at 4 kbar) and C-films before and after annealing at different temperatures.

Sample	Pellets		C-films		
	T/°C	*d*/g cm^{-3}	*T*/ °C	Doping	*d*/g cm^{-3}
1	–	0.75	–	–	0.18
	500	0.72	300	–	0.28
	1000	0.76	800	–	0.72
2	–	0.91	1000	–	1.00
	800	0.90	–	P	0.27
	1000	1.00	300	P	0.36
3	–	0.88	500	P	0.52
	1000	1.02	1000	P	0.91

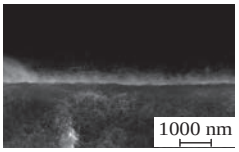

Figure 4 SEM image of the end cleavage for undoped nanocrystalline silicon C-film annealed at 1000 °C.

films initially possess low density, however it can be increased by a factor of 4–5 upon annealing in a high vacuum at temperatures up to 1000 °C. We associate the initial low density with agglomerates present in the sols of nanosilicon in polar solvents.[19]

This work was supported by the Russian Foundation for Basic Research (grant no. 17-03-01269).

Online Supplementary Materials

Supplementary data associated with this article can be found in the online version at doi: 10.1016/j.mencom.2020.07.041.

References

1 A. Waseda, K. Fujii and N. Taketoshi, *IEEE Trans. Instrum. Meas.*, 2005, **54**, 882.
2 D. Schneider and T. Schwarz, *Surf. Coat. Technol.*, 1997, **91**, 136.
3 P. Firth and Z. C. Holman, *ACS Appl. Nano Mater.*, 2018, **1**, 4351.
4 H.-F. Xiang, Z.-X. Xu, V. A. L. Roy, C.-M. Che and P. T. Lai, *Rev. Sci. Instrum.*, 2007, **78**, 034104.
5 W.-K. Chu, J. W. Mayer and M.-A. Nicolet, *Backscattering Spectrometry*, Academic Press, New York, 1978.
6 E. Ortel, A. Hertwig, D. Berger, P. Esposito, A. M. Rossi, R. Kraehnert and V.-D. Hodoroaba, *Anal. Chem.*, 2016, **88**, 7083.
7 I. Prencipe, D. Dellasega, A. Zani, D. Rizzo and M. Passoni, *Sci. Technol. Adv. Mater.*, 2015, **16**, 025007.
8 M. Tian, O. Dyck, J. Ge and G. Duscher, *Ultramicroscopy*, 2019, **196**, 154.
9 E. Chason and T. M. Mayer, *Crit. Rev. Solid State Mater. Sci.*, 1997, **22**, 1.
10 F. Voigt, R. Brüggemann, T. Unold, F. Huisken and G. H. Bauer, *Mater. Sci. Eng., C*, 2005, **25**, 584.
11 G. Nava, F. Fumagalli, S. Neutzner and F. Di Fonzo, *Nanotechnology*, 2018, **29**, 465603.
12 R. J. Anthony, K.-Y. Cheng, Z. C. Holman, R. J. Holmes and U. R. Kortshagen, *Nano Lett.*, 2012, **12**, 2822.
13 W. M. Visscher and M. Bolsterli, *Nature*, 1972, **239**, 504.
14 B. Abeles, H. L. Pinch and J. I. Gittleman, *Phys. Rev. Lett.*, 1975, **35**, 247.
15 Z. C. Holman and U. R. Kortshagen, *Nanotechnology*, 2010, **21**, 335302.
16 N. N. Kononov, G. P. Kuz'min, A. N. Orlov, A. A. Surkov and O. V. Tikhonevich, *Semiconductors*, 2005, **39**, 835 (*Fiz. Tekh. Poluprovodn.*, 2005, **39**, 868).
17 S. S. Bubenov, S. G. Dorofeev, A. A. Eliseev, N. N. Kononov, A. V. Garshev, N. E. Mordvinova and O. I. Lebedev, *RSC Adv.*, 2018, **8**, 18896.
18 N. Wang, Y. H. Tang, Y. F. Zhang, C. S. Lee, I. Bello and S. T. Lee, *Chem. Phys. Lett.*, 1999, **299**, 237.
19 S. Zhou, Z. Ni, Y. Ding, M. Sugaya, X. Pi and T. Nozaki, *ACS Photonics*, 2016, **3**, 415.

Received: 14th January 2020; Com. 20/6109